International Journal of Bifurcation and Chaos, Vol. 26, No. 5 (2016) 1650080 (11 pages)

DOI: 10.1142/S0218127416500802

Optoelectronic Chaos in a Simple Light Activated Feedback Circuit

K. L. Joiner
Nonlinear Dynamical Systems Group,*
Computational Science Research Center and
Department of Mathematics and Statistics,
San Diego State University, San Diego,
California 92182-7720, USA
kjoiner@rohan.sdsu.edu

F. Palmero
Nonlinear Physics Group,
Escuela Técnica Superior de Ingeniería Informática,
Departamento de Física Aplicada I,
Universidad de Sevilla, Avenida Reina Mercedes s/n,
41012 Sevilla, Spain
palmero@us.es

R. Carretero-González
Nonlinear Dynamical Systems Group,*
Computational Science Research Center and
Department of Mathematics and Statistics,
San Diego State University, San Diego,
California 92182-7720, USA
rcarretero@mail.sdsu.edu

Received September 4, 2015; Revised November 13, 2015

The nonlinear dynamics of an optoelectronic negative feedback switching circuit is studied. The circuit, composed of a bulb, a photoresistor, a thyristor and a linear resistor, corresponds to a nightlight device whose light is looped back into its light sensor. Periodic bifurcations and deterministic chaos are obtained by the feedback loop created when the thyristor switches on the bulb in the absence of light being detected by the photoresistor and the bulb light is then looped back into the nightlight to switch it off. The experimental signal is analyzed using tools of delay-embedding reconstruction that yield a reconstructed attractor with fractional dimension and positive Lyapunov exponent suggesting chaotic behavior for some parameter values. We construct a simple circuit model reproducing experimental results that qualitatively matches the different dynamical regimes of the experimental apparatus. In particular, we observe an order-chaos-order transition as the strength of the feedback is varied corresponding to varying the distance between the nightlight bulb and its photo-detector. A two-dimensional parameter diagram of the model reveals that the order-chaos-order transition is generic for this system.

Keywords: Optoelectronic device; nonlinear feedback; chaos.

*URL: http://nlds.sdsu.edu/

1. Introduction

Optoelectronic devices find diverse applications in telecommunications, military services, the medical field, and automatic control systems [Cuomo & Oppenheim, 1993; Almehmadi & Chatterjee, 2015]. In particular, sophisticated chaos-based communication systems have grown in popularity in recent years and are used to encrypt highly sensitive signals via chaos control techniques before their transmission over telecommunication channels [Apostolos *et al.*, 2005; VanWiggeren & Roy, 1998]. Due to the wide range of applications, chaotic signal phenomena have been extensively studied by employing various generation techniques such as propagation delay and feedback [Romeira *et al.*, 2014; Kouomou *et al.*, 2005]. In this paper, we study the generation of optoelectronic chaos via a nightlight subjected to negative feedback. First, even though optoelectronic devices have a wide relevance in science and technology there are few basic laboratory systems for which their complexity can be readily studied [Larger & Dudley, 2010]. Secondly, several of the chaos generation schemes in the literature above use large optical fiber feedback lines and sophisticated modulation devices to generate complex signals. We show through experiment and numerical analysis that the nightlight chaotic dynamics only depends on short feedback distances and circuit sensitivity allowing for easy control and prediction of its complex nature. These qualities demonstrate a basic light activated circuit which can be a viable system to employ in the generation and study of chaotic optoelectronic signals.

We chose to study a common household light activated nightlight manufactured by Meridian Electric Company (model 10400). As illustrated in Fig. 1, a feedback loop produces flickering as the bulb's light is detected by the internal CdS photoresistor and is fed back to redrive the nonlinear modulation of the wall mains input signal. Although nightlight flicker was noted in [James, 1996] the examination of the dynamics of the system did not go further than a few observations and measurements. This paper will be dedicated to a more in-depth study of the optoelectronic phenomena in this system and will be structured as follows. In Sec. 2, we provide experimental results of the chaotic dynamics of the nightlight system motivating our study. Section 3 presents the nightlight model including models for the tungsten bulb, CdS photoresistor and thyristor along with their parameter fitting. Also in this section, we present results of numerical simulations mapping the devices parameter space and examination of its deterministic nature. The paper concludes with a summary of results and possible avenues for further research.

2. Experimental Setup and Results

Figure 1 shows a sketch of the laboratory setup used to observe the nightlight feedback dynamics. To closely study the effects of the distance between the CdS photoresistor and the bulb, wire extensions are soldered between the photoresistor and its nodal connections to the nightlight circuit, which will be described in detail later. An AC voltage is fed to the nightlight from the wall mains and the light emitted from the tungsten bulb is captured using a photodiode. The photodiode is connected to an Rigol DS2000 digital oscilloscope which was used to observe and record the various output waveforms of the system.

2.1. *Delay-embedding reconstruction*

From the experimental data, it is in principle possible to reconstruct the dynamics of the system by time-delay embedding reconstruction [Kantz & Schreiber, 2003]. The selection of an appropriate time delay, τ, plays a critical role in correctly computing a systems correlation dimension from its time series. Time-delayed mutual information was suggested by [Fraser & Swinney, 1986] and applied in [Paula & Savi, 2015] as a tool to determine a reasonable τ and is given by the first minimum of the mutual information function

$$I = -\sum_{ij}^{N} p_{ij} \log \frac{p_{ij}(\tau)}{p_i p_j}. \tag{1}$$

In the above equation, for some partition on the real numbers, p_i is the probability to find a time series value in the ith interval, and $p_{ij}(\tau)$ is the joint probability that an observation falls into the ith

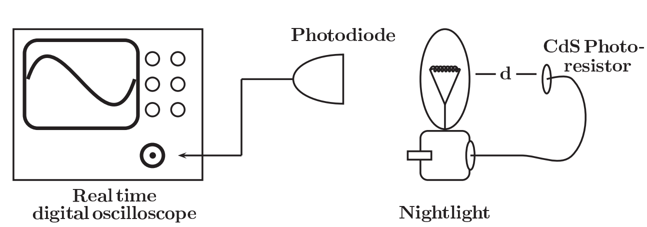

Fig. 1. Setup of the experimental nightlight system.

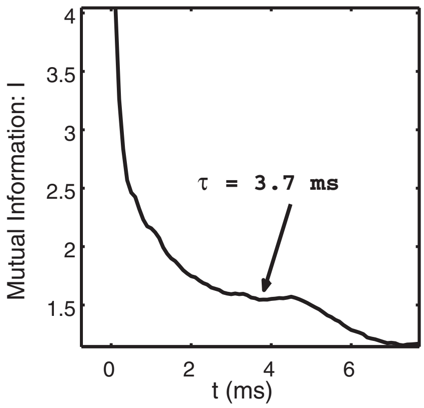

Fig. 2. Mutual information of the data corresponding to the nonperiodic dynamics depicted in Fig. 5(c).

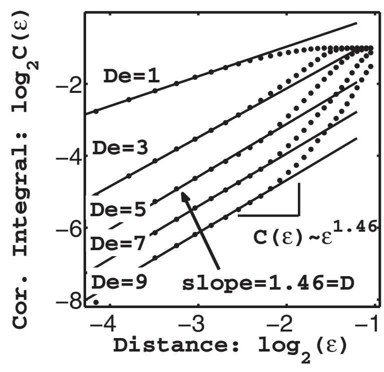

(a)

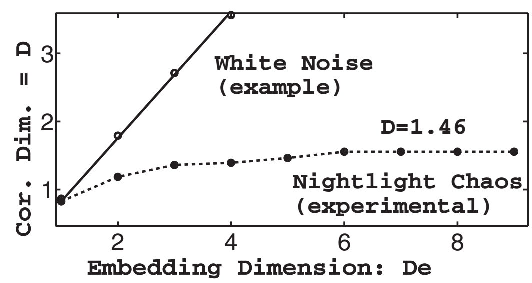

(b)

Fig. 3. Calculation of (a) correlation integral $C(r)$ and (b) correlation dimension D from the state corresponding to Fig. 5(c).

interval and the observation time τ later falls into the jth. Figure 2 shows that the first minimum of mutual information of the experimental data computed with Eq. (1) occurs around $\tau = 3.7\,\text{ms}$.

The correlation dimension D of the attractor corresponding to the nonperiodic dynamics depicted in Fig. 5(c) is computed using [Alligood *et al.*, 1996]

$$D = \lim_{r\to 0} \frac{\log C(r)}{\log r},$$

where $C(r)$ is the correlation integral with respect to an arbitrary distance r and is given by

$$C(r) = \frac{1}{N_s^2} \sum_{i,j=1}^{N_s} H(r - |\mathbf{x}_i - \mathbf{x}_j|) \sim r^D,$$

where H is the Heaviside function, $\mathbf{x}_{i,j}$ are points on the attractor and N_s is the number of sample points. As shown in Fig. 3, D was obtained by increasing the embedding dimension, D_e, until D converged to the intrinsic dimension of the attractor which was found to be $D = 1.46$. The fractal dimension of the attractor is a indicator of chaos.

As shown in Fig. 3(b), the correlation dimension begins to plateau at $D_e = 3$ which implies an embedding of the orbit into a three-dimensional state space $\{P(t), P(t+\tau), P(t+2\tau)\}$. Figure 4 displays the reconstructed attractor from the experimental time series depicted in Fig. 5(c) and shows the feedback system does not converge to a closed orbit but instead into a "strange attractor".

2.2. *Chaotic behavior*

Figure 5 demonstrates how the bulb's output waveform and power spectra evolve as nonlinear feedback is introduced into the system by pointing the CdS photoresistor at the tungsten bulb at various distances, d, from the bulb. In Figs. 5(a) and 5(b), as d is decreased from 4.5 cm to 4.25 cm

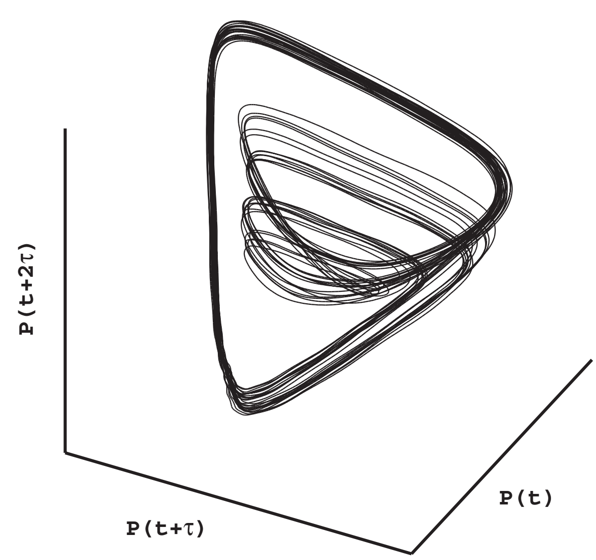

Fig. 4. Reconstruction of the attractor from the state in Fig. 5(c) using delay coordinates depicted as embedded in three-dimensional phase space ($\tau = 3.7\,\text{ms}$).

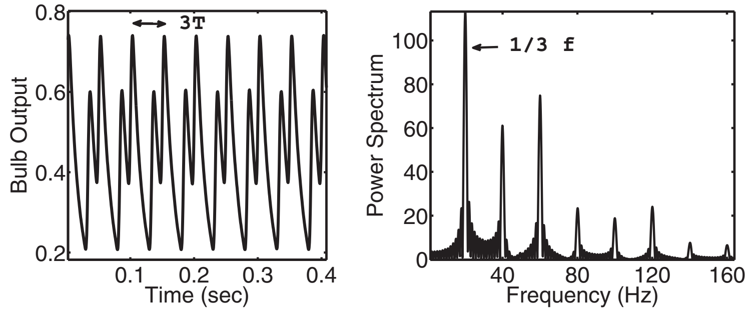

(a) Period $3T$ $d = 4.5\,\mathrm{cm}$

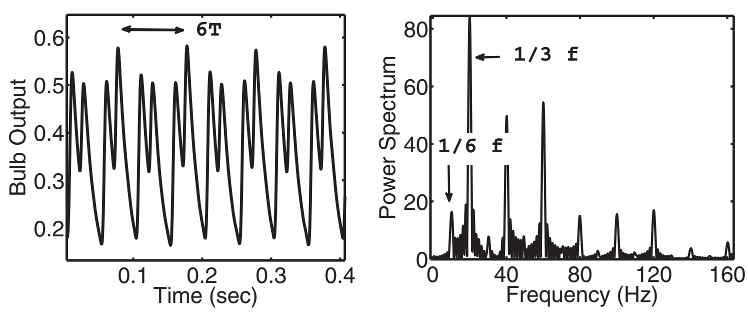

(b) Period $6T$ $d = 4.25\,\mathrm{cm}$

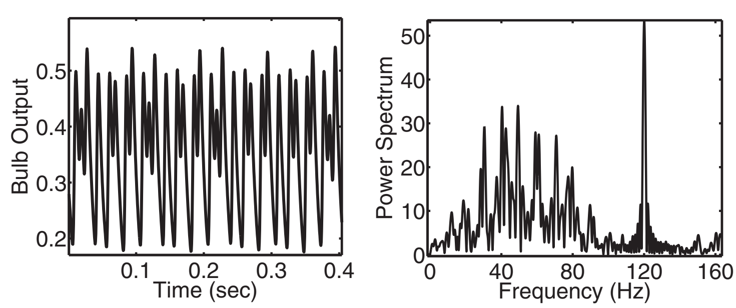

(c) Chaos $d = 4.0\,\mathrm{cm}$

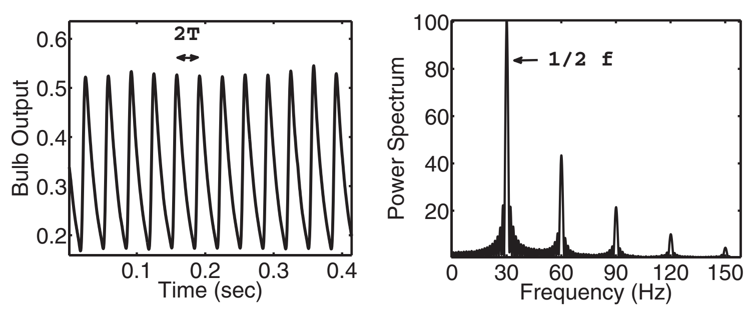

(d) Period $2T$ $d = 3.9\,\mathrm{cm}$

Fig. 5. Waveforms from the nightlight experiment. The left panels show the output waveforms when feedback is introduced to the system at various distances between approximately 4.5 cm to 4.0 cm. The right panels display the corresponding power spectra depicting a period-doubling route to chaos.

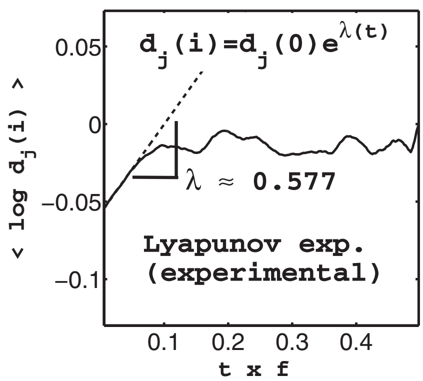

Fig. 6. Average exponential growth computed from the experimental time series corresponding to the state in Fig. 5(c), namely, when $d = 4\,\text{cm}$. The linear fit to the first portion of the data gives an estimated Lyapunov exponent of $\lambda \approx +0.577$. Note that for longer times the separation distance saturates as the attractor has finite size. Time has been rescaled by the frequency of the wall mains $f = 60\,\text{Hz}$.

the left panels show the waveforms initial period of $3T$, where $T = 1/f$ is the period of the wall mains, bifurcates to a period of $6T$. The $f/3$ and $f/6$ frequency components are clearly seen in the corresponding power spectra in the right panels. As shown in Fig. 5(c), at $d = 4.0$ cm the feedback system transitions to a state with more complex waveforms and appear to lose periodicity. The power spectrum is wide, suggesting the system behaves chaotically in this regime. Finally, Fig. 5(d) shows that the output signal transitions back into a regular periodic state of period $2T$. This suggests an order-chaos-order transition as the distance d is varied (see below for further details).

In order to verify the system's chaotic dynamics, the largest Lyapunov exponent λ for the time series was estimated using a method well suited for small data sets [Rosenstein *et al.*, 1993]. Figure 6 shows a least-squares fit to the averaged linear relationship defined by

$$y(i) = \frac{1}{\Delta t}\langle \log d_j(i) \rangle,$$

where Δt is the sampling period, $d_j(i)$ is the distance between the jth pair of nearest neighbors after i discrete-time steps and $\langle\cdot\rangle$ denotes the average over all values of j. Figure 6 depicts the average growth of $\langle \log d_j(i) \rangle$ for the experimental data corresponding to $d = 4\,\text{cm}$ [see Fig. 5(c)]. As it is clear from the figure, the growth is, for short times, approximately linear which yields an estimated value for the largest Lyapunov exponent of $\lambda \approx +0.577$ where time has been rescaled to the natural frequency of the system given by the frequency of the wall mains ($f = 60\,\text{Hz}$) that drive (force) the circuit. This result gives a clearly positive value for λ which is characteristic of chaotic dynamics. This further supports the results above that also suggested that the experimental circuit is chaotic for $d = 4\,\text{cm}$.

3. Numerical Model and Results

3.1. *Model*

Upon disassembling the nightlight one can observe the circuit layout depicted in Fig. 7. The device is driven by the household mains, labeled V_{in}, with a root mean square (rms) voltage of 110 V and a 60 Hz frequency. The tungsten bulb, B, has a 4 W power rating and is triggered on in the dark and is triggered off when light is sensed by the CdS photocell denoted as R_{ph}. The circuit also contains a thyristor along with a linear resistor, R, which determines the circuit's sensitivity to light. Let us now model the different components included in the nightlight circuit: the bulb, the photoresistor, and the thyristor.

3.1.1. *Source*: *Tungsten bulb*

In [Hu & Lucyszyn, 2015; Clauss *et al.*, 2001] tungsten bulb models were analyzed both experimentally and numerically based on the Stephan–Boltzmann law and assuming the filament input power must be equal to its radiated output power in thermal equilibrium. Similarly, taking the bulb electrical voltage to be, v_B, over time, t, the model

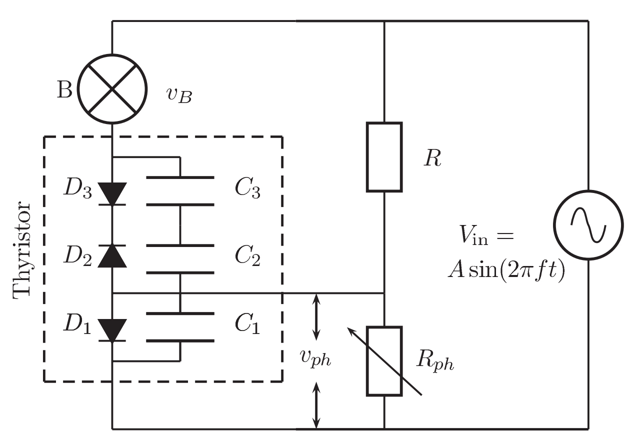

Fig. 7. The nightlight circuit. The circuit is composed of a light bulb B, a thyristor, a linear resistor R and the photoresistance R_{ph}. The system is connected to a sinusoidal voltage source V_{in} of amplitude A and frequency f.

we use for the bulb is

$$MC(T)\frac{dT}{dt} = \frac{v_B^2(t)}{R_f(T)} - \sigma(T^4 - T_0^4). \tag{2}$$

The variable T represents the filament temperature in degrees Kelvin, $C(T)$ is the heat capacity of tungsten and $R_f(T)$ is the filament temperature dependent resistance. The parameters M and σ are used to fit the model to an ideal 4 W light-bulb and represent the filament's effective mass and constant of proportionality between radiative intensity and temperature.

In [Forsythe & Worthing, 1925] the resistance and temperature of a tungsten filament are shown to be related by the following expression

$$R_f(T) = R_0\left(\frac{T}{T_0}\right)^{1.2}, \tag{3}$$

where R_0 is the resistance of tungsten at room temperature and T_0 is room temperature in degrees Kelvin. We measured the value for R_0 using an ohmmeter. A modeling value for σ was determined by assuming an average electromagnetic radiative power output of 4 W in thermal equilibrium ($dT/dt = 0$) with an average applied voltage of $V(t) = 110\,\text{V}$.

Manufacturing specifications gives the tungsten bulb's operating temperature to be $\approx 2200°\text{K}$. The parametrization of the heat capacity for tungsten in the temperature range of 0–3000°K is taken to be

$$C(T) = 3R_g\left(1 - \frac{\Theta_D^2}{20T^2}\right) + 2aT + 4bT^3,$$

where R_g is the gas constant, Θ_D is the Debye temperature, $a = 4.5549 \times 10^{-3}$ and $b = 5.77874 \times 10^{-10}$, [Yih & Wang, 1979]. The linear term a represents the contribution from electronic specific heat and b reflects the influence of any anharmonic vibrations within the tungsten compound [Hoch & Vernardakis, 1975].

3.1.2. *Passive nonlinearity*: *Photoresistor*

The photoresistor is a semiconductor device that converts light into an electrical signal, such as voltage or current, which is precisely the feedback control at the heart of the nightlight device. Recent computer-assisted experiments show photoresistors are sensitive and exhibit a fast, nonlinear response to light signals [Kraftmakher, 2012]. For the current project we describe the photoresistor's transient carrier density, N, by [Pierret & Neudeck, 1988]

$$\frac{dN}{dt} = \Re I_{\text{wave}}(t) - \frac{N}{\tau_e}, \tag{4}$$

where τ_e is the semiconductor carrier recombination lifetime and $\Re$ is its sensitivity to the incident optical power; $I_{\text{wave}}(t)$. The main property of the photoresistor is expressed by its resistance under illumination as $R_{ph} \propto I_{\text{wave}}^{-1}$ [Saleh & Teich, 1991]. We introduce the scaling $N = \Re n$ to simplify Eq. (4) and express our photoresistor model compactly as

$$\frac{dn}{dt} = I_{\text{wave}}(t) - \frac{n}{\tau_e}, \tag{5}$$

$$R_{ph} = \frac{c}{n^{\psi}}. \tag{6}$$

The parameters c and ψ were determined by taking measurements of resistance of the photoresistor while varying the distance, d, between the tungsten bulb and the photoresistor and is shown in Fig. 8.

3.1.3. *Active nonlinearity*: *Thyristor*

A thyristor conducts current only in the forward direction, can block voltage in both directions, turns on when a firing pulse is provided and turns off when the thyristor current becomes zero. A physically accurate, but computationally stiff, lumped diode model of the thyristor was designed in [Chua *et al.*, 1987] and implemented in [Hoh & Yasuda, 1994] with static (I_A, V_{AK}) characteristics approximated by a piecewise-linear function. Similarly, our modeling approach is to form approximate expressions for the bulb and photoresistor voltages based on an approximate model of the thyristor.

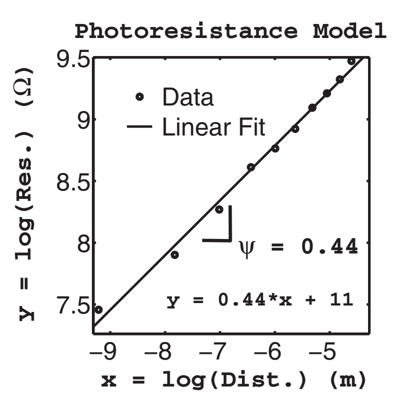

Fig. 8. The CdS photoresistor response to incident light. Depicted is the log–log plot of the photoresistor resistance versus the distance to a 4 W light source.

By assuming the thyristor produces a rectified wave conducting the lower half cycles of the supply voltage across its pn junction diodes and the upper half cycle across the bulb, v_B can be modeled as

$$v_B = \frac{V_{\text{in}} + v_f - |V_{\text{in}} - v_f|}{2}.$$

Using the above expression for v_B, a nodal analysis of the circuit diagram in Fig. 7 allows its switching dynamics to be conveniently described in the following algorithm:

Algorithm: `CIRCUIT STATE` (v_{ph}, I_h)

if $v_{ph} > v_t$ (Thyristor on)

$$v_B = \frac{V_{\text{in}} + v_f - |V_{\text{in}} - v_f|}{2},$$

$$v = V_{\text{in}} - v_B,$$

$$v_{ph} = \frac{v\,R_{ph}}{R_{ph} + R}.$$

else if $I_h > 0$

$$v_B = \frac{V_{\text{in}} + v_f - |V_{\text{in}} - v_f|}{2},$$

$$v = V_{\text{in}} - v_B,$$

$$v_{ph} = \frac{v\,R_{ph}}{R_{ph} + R}.$$

else (Thyristor off)

$$v_B = 0,$$

$$v = \frac{V_{\text{in}}\,R_{ph}}{R_{ph} + R},$$

$$v_{ph} = v.$$

return v_B v_{ph}

The PCR606J data-sheet gives the thyristor gate triggering voltage as $v_t = 0.8\,\text{V}$, the holding current as $I_h = 5.0\,\text{mA}$ and the forward voltage as $v_f = 1.0\,\text{V}$. In order to test the robustness of our thyristor model a low voltage replica of the nightlight circuit was constructed and data collected on the thyristor voltage, v_{ak}, with the photoresistor under two states of illumination. The results are displayed in Fig. 9 which show good agreement between the data and the model.

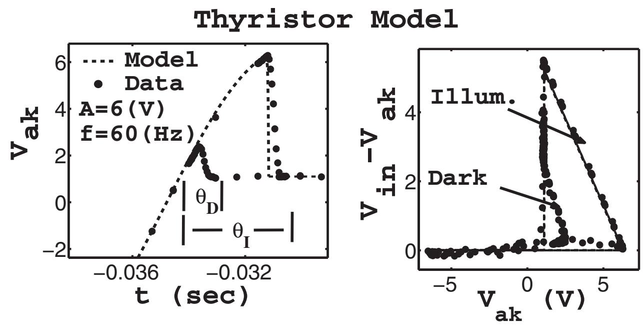

Fig. 9. Simulation versus data of the thyristor when the circuit is in different states of illumination. Left: In darkness the thyristor has a small conduction angle, θ_D, relative to θ_I when under illumination. Right: The thyristor representative (i–v) curve depicts distinct regions of negative differential conductivity under illumination (Illum) and darkness (Dark).

3.2. *Simulation*

Feedback is introduced into the model by setting $I_{\text{wave}} = \sigma(T^4 - T_0^4)/d^2$ (power/distance^2) and simulations are accomplished by numerically integrating the system:

$$MC(T)\frac{dT}{dt} = \frac{v_B(t)^2}{R_f(T)} - \sigma(T^4 - T_0^4),$$

$$\frac{dn}{dt} = I_{\text{wave}}(t) - \frac{n}{\tau_e},$$

where the state of $v_B(t)$ is determined by events given by the conditions of the `CIRCUIT STATE` algorithm defined above. The simulation is accomplished in a series of time intervals with initial conditions (T_0, n_0) given from the final values (T_f, n_f) of the systems' previous state. For clarity, the meaning and values of the physical and modeling parameters are listed in Table 1.

3.3. *Parameter space and dynamics of the model*

The dynamics of the system is studied by varying the linear resistor and distance parameters R and d. Figure 10 depicts, in the parameter space (d, R), the regions where the output waveform is periodic (with periods T, $2T$, and $3T$) and where it is chaotic. The figure was obtained by sweeping d for fixed values of R (at intervals of $0.5\,\text{M}\Omega$) and determining the state of the system by observing the power spectrum of the simulated bulb output, $P(t)$, calculated as

$$P(t) = \sigma(T^4 - T_0^4).$$

Table 1. Definitions of the physical and modeling parameters of the nightlight feedback system.

Parameter	Value	Meaning
A	110 V	Mains amplitude
f	60 Hz	Mains frequency
T_0	274.15 K	Room temperature
R_0	250 Ω	W Resistance at T_0
R_g	45.23 J/K mol	W Gas constant
Θ_D	310 K	Debye temperature
σ	1.74×10^{-13}	Bulb model parameter 1
M	1×10^{-6} kg	Bulb model parameter 2
τ_e	1×10^{-12} s	Carrier lifetime
c	0.454	CdS model parameter 1
ψ	0.44	CdS model parameter 2
v_f	1.7 V	Thyristor forward voltage
i_h	5.0 mA	Thyristor holding current

The parameter space shows a thin "critical strip" where chaotic feedback dynamics occur over a range of sensitivities and feedback distances. Figure 10 predicts as the circuit is made more sensitive to light (by increasing R) then the system's switching phenomena occurs at larger distances thus illustrating the two parameters' interdependence.

To illustrate the effects that R has on the quality of dynamics exhibited by the system, simulations were performed while keeping d constant and varying R along the vertical line depicted in Fig. 10. For each value of R, the crest factor, C_i, of each

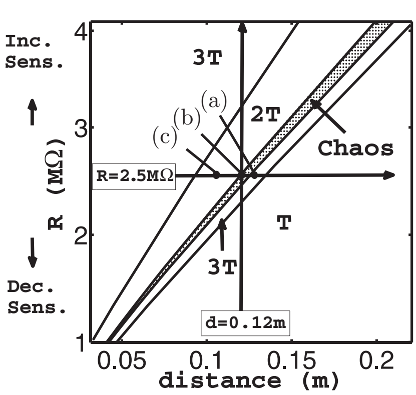

Fig. 10. Two-dimensional parameter space (d, R) for the numerical model. The different regions correspond to periods T, $2T$, and $3T$ and to chaotic orbits (shaded area). The three points labeled (a)–(c) depict the parameter values used for the waveforms and power spectra in Fig. 13. The model predicts that increasing/decreasing R should result in a corresponding increase/decrease in circuit sensitivity and a shift in the value of d required for chaos.

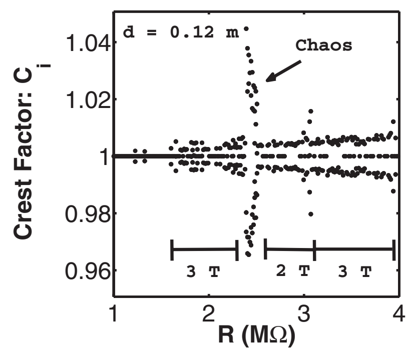

Fig. 11. Crest factor of the model's power output corresponding to the strip $d = 0.12$ m in Fig. 10.

peak, pk_i, of the output waveform was computed as

$$C_i = \frac{pk_i}{pk_{\mathrm{rms}}},$$

where $pk_{\mathrm{rms}} = \sqrt{(pk_1^2 + pk_2^2 + \cdots + pk_n^2)}/n$ is the root mean square of the set of peaks $\{pk_i\}$, $(i = 1, \ldots, n)$. Figure 11, depicting the crest factor

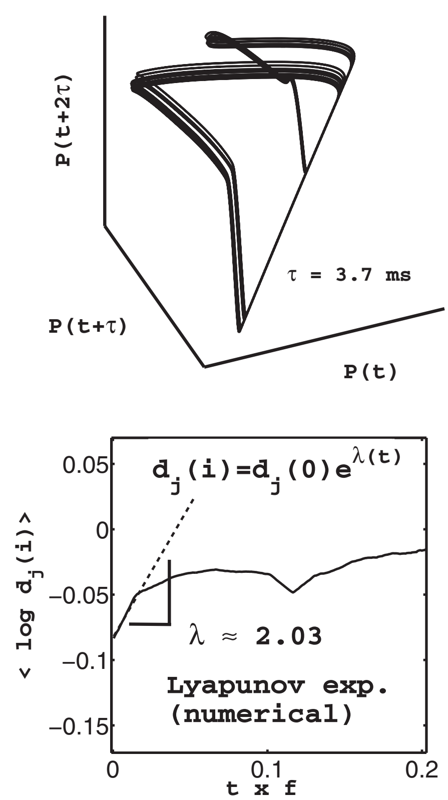

Fig. 12. Top panel: Reconstructed attractor of the circuit model from the chaotic region of Fig. 11. Bottom panel: Average exponential growth computed from the numerical time series corresponding to the chaotic state in Fig. 13(b). The linear fit estimates a largest Lyapunov exponent of $\lambda = +2.03$. For both panels the model parameters are $R = 2.5\,\mathrm{M\Omega}$ and $d = 0.12$ cm.

dependence on R, clearly shows the effect of R on the system's route to chaos. The peaks of the waveform remain quasi-periodically concentrated near their rms value and diverge when the system is in its chaotic regime. Interestingly, in Fig. 11 there seems to be a transition from order to chaos to order as one sweeps the resistance R.

Figure 12 shows the bulb output of the simulated waveform in the chaotic region depicted in Fig. 11 embedded in three dimensions with the same time delay $\tau = 3.7\,\text{ms}$ as the experimental data from Fig. 4 and, correspondingly, displays the system's fractal structure. Finally, the largest Lyapunov exponent of the numerical attractor was computed using the same method as the one used for Fig. 6 which yields a value of $\lambda = +2.03$ which demonstrates that the model can reproduce chaotic dynamics by adjusting R while holding d fixed. It is important to note that the qualitative behavior of the system does not depend on the precise value of R (as different "cuts" for fixed R seem to produce qualitatively the same order-chaos-order transition; see Fig. 10). This is a strong indication that the phenomena hereby described — cf. period bifurcations and chaos — is generic. For instance, the incorporation of small amounts of noise should not affect the qualitative characteristics of the system.

Finally, to compare the qualitative dynamics of the model to the experimental results, we present in Fig. 13 the waveforms and their power spectra

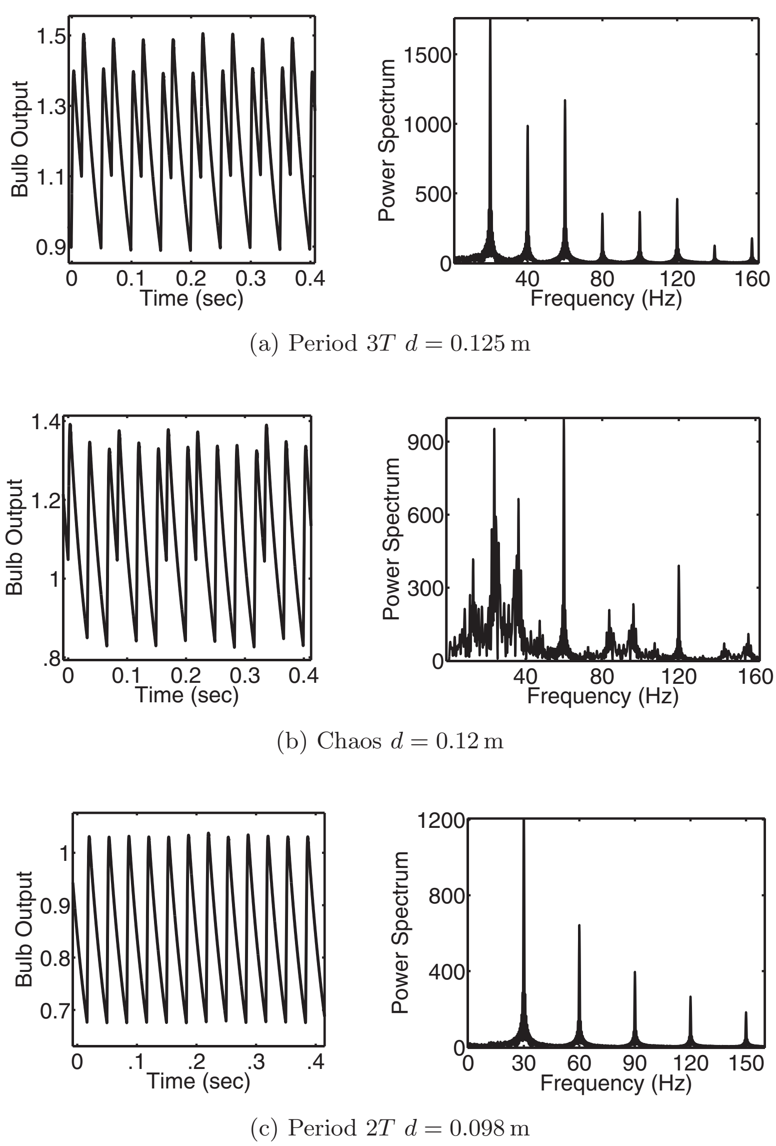

Fig. 13. Waveforms (left panels) and their corresponding power spectra (right panels) of the circuit model at the points (a)–(c) labeled in Fig. 10.

for our model corresponding to the $3T$, chaos, and $2T$ experimental cases of Fig. 5. As it is evidenced from the figure, the waveforms obtained from the model have a striking resemblance to the waveforms from the experiments. Specifically, the power spectra reveal similar characteristics between the theoretical and experimental waveforms. Note that in Fig. 13 we chose a range of values for the linear resistor R larger than the corresponding one in our experiment (approximatively $1\,\mathrm{M}\Omega$) in order to demonstrate the robustness of the order-chaos-order transition. The system output and power spectra for $R = 1\,\mathrm{M}\Omega$ are similar to the ones corresponding to the experiment (see Fig. 5).

4. Conclusions

The feedback behavior of a nightlight circuit was studied. We presented experimental results where the light emanating from a nightlight was fed back into itself. This created a feedback loop as the nightlight turns on in the absence of light, but as it turns on, it produces light that is fed back into itself inducing its dimming down. We showed that this feedback loop does not induce a stable equilibrium but induces bifurcations in the period as the feedback strength is varied by adjusting the distance between the nightlight bulb and its light detecting photoresistor. As this distance is decreased, the output signal of the bulb undergoes period bifurcation until it exhibits apparently chaotic dynamics. Decreasing further the distance resulted in regularization of the dynamics thus giving an order-chaos-order transition as the distance is varied.

The behavior of the system was explained by taking into account the influence of the feedback distance and the linear resistor effect on system sensitivity. Observing the power spectra of the bulb's output signal showed waveforms consisting of a mixture of frequencies which resulted in complex aperiodic behavior. Our model is based on a commercially available nightlight device that contains a photoresistor, a thyristor and a linear resistor. The obtained model was able to predict qualitatively the bifurcations observed in the experiment, including the order-chaos-order transition as the strength of the feedback is varied. Very good qualitative agreement was observed between the experimental results and the numerics ensuring for our model for the different types of periodic and apparently chaotic dynamics. The nonperiodic dynamics in the experiment was analyzed by delay-embedding attractor reconstruction and the computation of its corresponding correlation dimension. We obtained a correlation dimension of $D = 1.46$ evidencing the fractal nature of the attractor. Furthermore, we also computed, from the reconstructed dynamics, the largest Lyapunov exponent yielding a value of $\lambda = 0.577$ and thus confirming that the dynamics is indeed chaotic. The power spectra of the output signals in the different regimes also suggested that for intermediate distances between the bulb and the photoresistor the dynamics was chaotic. Qualitatively similar conclusions were also obtained for the corresponding model including, remarkably, the order-chaos-order transition.

Furthermore, a two-dimensional parameter phase transition diagram of the model showed that the observed order-chaos-order transition was generic. We note that although the chaotic region seems to be generic, it is relatively thin and therefore some care is necessary to obtain conditions for its manifestation. This was also observed in the experiments where apparently aperiodic behavior could be obtained by slowly varying (decreasing) the distance between the bulb and the photoresistor for a narrow window of distances.

The physical mechanisms underlying the critical distance between the nightlight's bulb and the ensuing output phenomena remains unknown. Achieving a deeper understanding of its properties would require close investigation of the circuits' nonlinear devices under operation. Thus, it would be interesting to expand the present considerations of negative feedback signals to a more sophisticated and measurable chaos generation system incorporating a similar light activated circuit in order to examine its operating dynamics in finer detail. It may be possible to conduct experiments and simulations with chaos control techniques to yield insight into understanding the control of chaotic optoelectronic signals and encryption techniques and devices.

References

Alligood, K. T., Sauer, T. D. & Yorke, J. A. [1996] *Chaos: An Introduction to Dynamical Systems* (Springer, NY).

Almehmadi, F. S. & Chatterjee, M. R. [2015] "Secure chaotic transmission of electrocardiography signals with acousto-optic modulation under profiled beam propagation," *Appl. Opt.* **54**, 195–203.

Apostolos, A., Dimitris, S., Laurent, L., Valerio, A., Pere, C., Ingo, F., Jordi, G., Claudio, R. M., Luis, P. & Alan, S. [2005] "Chaos-based communications at high bit rates using commercial fibre-optic links," *Nature* **438**, 343–346.

Chua, L. O., Desoer, C. A. & Kuh, E. S. [1987] *Linear and Nonlinear Circuits* (McGraw-Hill, USA).

Clauss, D. A., Ralich, R. M. & Ramsier, R. D. [2001] "Hysteresis in a light bulb: Connecting electricity and thermodynamics with simple experiments and simulations," *Eur. J. Phys.* **22**, 385–394.

Cuomo, K. M. & Oppenheim, A. V. [1993] "Circuit implementation of synchronized chaos with applications to communications," *Phys. Rev. Lett.* **71**, 65–68.

Forsythe, W. E. & Worthing, A. G. [1925] "The properties of tungsten and the characteristics of tungsten lamps," *Astrophys. J.* **61**, 146–185.

Fraser, A. M. & Swinney, H. L. [1986] "Independent coordinates for strange attractors from mutual information," *Phys. Rev. A* **33**, 7306–7312.

Hoch, M. & Vernardakis, T. [1975] "Specific heat and thermal expansion of solids at high temperature," *Scripta Metall. Mater.* **9**, 1131–1133.

Hoh, K. & Yasuda, Y. [1994] "Electronic chaos in silicon thyristor," *Jpn. J. Appl. Phys.* **33**, 594–598.

Hu, F. & Lucyszyn, S. [2015] "Modelling miniature incandescent light bulbs for thermal infrared THz torch applications," *J. Infrared Millim. Te.* **36**.

James, G. E. [1996] "Chaos theory, the essentials for military applications," *NWC Newport Paper* **10**, 20–27.

Kantz, H. & Schreiber, T. [2003] *Nonlinear Time Series Analysis* (Cambridge University Press, Cambridge).

Kouomou, Y. C., Colet, P., Larger, L. & Gastaud, N. [2005] "Chaotic breathers in delayed electro-optical systems," *Phys. Rev. Lett.* **95**, 1–4.

Kraftmakher, Y. [2012] "Experiments on photoconductivity," *Eur. J. Phys.* **33**, 503–511.

Larger, L. & Dudley, J. M. [2010] "Optoelectronic chaos," *Nature* **465**, 41–42.

Paula, A. S. & Savi, M. A. [2015] "State space reconstruction applied to a multiparameter chaos controlled method," *Meccanica* **50**, 207–216.

Pierret, R. F. & Neudeck, G. W. [1988] *Semiconductor Fundamentals* (Addison-Wesley, NY).

Romeira, B., Kong, F., Li, W., Figueiredo, J. M., Javaloyes, J. & Yao, J. [2014] "Broadband chaotic signals and breather oscillations in an optoelectronic oscillator incorporating a microwave photonic filter," *J. Lightw. Technol.* **32**, 3933–3940.

Rosenstein, M. T., Collins, J. J. & De Luca Carlo, J. [1993] "A practical method for calculating largest Lyapunov exponents from small data sets," *Physica D* **65**, 117–134.

Saleh, B. E. & Teich, M. C. [1991] *Fundamentals of Photonics* (John Wiley and Sons, NY).

VanWiggeren, G. D. & Roy, R. [1998] "Optical communication with chaotic waveforms," *Phys. Rev. Lett.* **81**, 3547–3550.

Yih, S. W. H. & Wang, C. T. [1979] *Tungsten Sources, Metallurgy, Properties and Applications* (Springer, NY).